JOURNAL OF CELLULAR PHYSIOLOGY 206:655–663 (2006)

Over-Expression of Heme Oxygenase-1 Promotes Oxidative Mitochondrial Damage in Rat Astroglia

WEI SONG,[1] HAIXIANG SU,[1] SISI SONG,[1,2] HEMANT K. PAUDEL,[1,2] AND HYMAN M. SCHIPPER[1,2]*
[1]Lady Davis Institute for Medical Research, Jewish General Hospital, Montreal, Quebec, Canada
[2]Department of Neurology and Neurosurgery, McGill University, Montreal, Quebec, Canada

Glial heme oxygenase-1 is over-expressed in the CNS of subjects with Alzheimer disease (AD), Parkinson disease (PD) and multiple sclerosis (MS). Up-regulation of HO-1 in rat astroglia has been shown to facilitate iron sequestration by the mitochondrial compartment. To determine whether HO-1 induction promotes mitochondrial oxidative stress, assays for 8-*epi*$PGF_{2\alpha}$ (ELISA), protein carbonyls (ELISA) and 8-OHdG (HPLC-EC) were used to quantify oxidative damage to lipids, proteins, and nucleic acids, respectively, in mitochondrial fractions and whole-cell compartments derived from cultured rat astroglia engineered to over-express human (h) HO-1 by transient transfection. Cell viability was assessed by trypan blue exclusion and the MTT assay, and cell proliferation was determined by [^{3}H] thymidine incorporation and total cell counts. In rat astrocytes, hHO-1 over-expression ($\times$3 days) resulted in significant oxidative damage to mitochondrial lipids, proteins, and nucleic acids, partial growth arrest, and increased cell death. These effects were attenuated by incubation with 1 μM tin mesoporphyrin, a competitive HO inhibitor, or the iron chelator, deferoxamine. Up-regulation of HO-1 engenders oxidative mitochondrial injury in cultured rat astroglia. Heme-derived ferrous iron and carbon monoxide (CO) may mediate the oxidative modification of mitochondrial lipids, proteins and nucleic acids in these cells. Glial HO-1 hyperactivity may contribute to cellular oxidative stress, pathological iron deposition, and bioenergetic failure characteristic of degenerating and inflamed neural tissues and may constitute a rational target for therapeutic intervention in these conditions. J. Cell. Physiol. 206: 655–663, 2006. © 2005 Wiley-Liss, Inc.

On the basis of considerable experimental data adduced from whole animal and in vitro studies, the heme oxygenases have emerged as dynamic sensors of cellular oxidative stress and likely arbiters of net tissue redox homeostasis. Heme oxygenases are located within the endoplasmic reticulum where they serve, in concert with NADPH cytochrome P450 reductase, to oxidize heme to biliverdin, free ferrous iron, and carbon monoxide (CO). Biliverdin is metabolized further to the bile pigment, bilirubin by action of biliverdin reductase (Ewing and Maines, 1995; Ryter and Tyrrell, 2000). Mammalian cells express at least two isoforms of heme oxygenase, HO-1 (a.k.a. heat shock protein 32) and HO-2. A third protein, HO-3 may be a retrotransposition of the HO-2 gene unique to rats (Scapagnini et al., 2002). In the normal brain, basal HO-1 expression is low and restricted to small groups of scattered neurons and neuroglia (Baranano and Snyder, 2001). The *ho-1* gene is highly inducible by a host of pro-oxidant and inflammatory stimuli including heme, ß-amyloid, dopamine, kainic acid, H_2O_2, UV light, transition metals, prostaglandins, Th1 cytokines, and lipopolysaccharide (Matsuoka et al., 1998; Dennery, 2000; Schipper, 2000). In the face of oxidative challenge, induction of HO-1 may protect cells by augmenting the breakdown of pro-oxidant heme and hemoproteins to the radical-scavenging bile pigments, biliverdin, and bilirubin (Stocker et al., 1987; Nakagami et al., 1993; Llesuy and Tomaro, 1994; Dore et al., 1999; Baranano and Snyder, 2001). Conversely, in some tissues and under certain experimental conditions, heme-derived iron and CO may exacerbate intracellular oxidative stress and cellular injury by promoting free radical generation within the mitochondrial and other cellular compartments (Zhang and Piantadosi, 1992; Frankel et al., 2000).

Studies involving various whole animal and tissue culture models of CNS injury and disease have yielded conflicting evidence favoring HO-1-mediated cytoprotection in certain experimental paradigms (Chen et al., 2000) and neuroendangerment in others (Kadoya et al., 1995). In a given neuropathological condition, the extent and duration of HO-1 induction, the cell type of origin, and the status of the local redox microenvironment may determine whether the pro-oxidant potential of liberated iron/CO or the antioxidant benefits of a diminished heme:bilirubin ratio prevail (Galbraith, 1999).

We and others have demonstrated robust up-regulation of HO-1 mRNA or protein in astrocytes residing within human neural tissues affected by Alzheimer disease (AD), Parkinson disease (PD), multiple sclerosis (MS), and ischemia-reperfusion, as well as in animal models of these CNS disorders (reviewed in Schipper, 2004a,b). Moreover, experiments conducted in our laboratory revealed that up-regulation of HO-1 promotes mitochondrial sequestration of non-transferrin-derived iron in cultured rat astroglia. Taken together, these findings suggested that induction of the glial *ho-1* gene may contribute to the pathological iron sequestration and mitochondrial insufficiency amply documented in the brains of AD, PD, and MS patients (Schipper, 2004a,b). In cultured astrocytes, HO-1 over-expression provokes the compensatory up-regulation of the manganese superoxide dismutase (*mnsod*) gene suggesting

Contract grant sponsor: Valorisation-Recherche Québec (HMS, HP); Contract grant sponsor: Canadian Institutes of Health Research (HMS).

*Correspondence to: Hyman M. Schipper, Lady Davis Institute for Medical Research, SMBD Jewish General Hospital, 3755 Cote Ste. Catherine Road, Montreal, Quebec H3T 1E2, Canada.
E-mail: hyman.schipper@mcgill.ca

Received 20 July 2005; Accepted 26 July 2005

DOI: 10.1002/jcp.20509

that heme-derived free ferrous iron and CO exert pro-oxidant effects on the mitochondrial compartment (Frankel et al., 2000; Schipper, 2004b). In the present study, we sought direct evidence that up-regulation of the human (h) *ho-1* gene in cultured astroglia subjects the mitochondrial compartment to oxidative stress and determined the impact of hHO-1 over-expression on the viability and proliferative capacity of these cells.

MATERIALS AND METHODS

Materials

Neonatal Sprague–Dawley rats were obtained from Charles River Breeding Farms (St. Constant, Quebec, Canada). Ham's F-12, high glucose Dulbecco's modified Eagle's medium (DMEM), and opti-MEM I reduced serum medium were purchased from GIBCO BRL (Life Technologies, Burlington, Canada). Horse serum and fetal bovine serum were purchased from WISENT (St-Bruno, Canada), penicillin-streptomycin, HEPES, 4-(2-aminoethyl)-benzenesulfonyl fluoride hydrochloride (AEBSF), sodium fluoride, pepstatin A, aprotinin, leupeptin, monoclonal anti-Flag M2, and anti-β actin antibodies were obtained from Sigma Chemical Co. (St. Louis, MO). Tin mesoporphyrin (SnMP) was purchased from Porphyrin Product (Logan, UT). Tissue culture flasks (25 and 75 cm^2) and 6- and 24-well plates were obtained from Fisher Scientific Ltd. (Montreal, Canada). Human heme oxygenase-1 (*Xho*I-*Eco*RI) (1Kb) in pBluescript SKII(+) was obtained from Dr. S. Shibahara (Tohuku University, Japan), pcDNA3.1(+)/Zeo CMV Flag from Dr. R. Lin (Lady Davis Institute for Medical Research, Montreal, Quebec) and pEGFP.C1 from Clontech (Palo Alto, CA). Qiagen plasmid kits were obtained from Qiagen, Inc. (Chatsworth, CA), goat anti-mouse IgG and pGEM-T Easy Vector System from Promega (Madison, WI), [*methyl*-^{3}H] thymidine, restriction enzymes and ECL Western blotting reagents from Amersham Biosciences UK Ltd. (Buckinghamshire, England), Lipofectamine 2000 reagent from Invitrogen (Carlsbad, CA), Bradford reagent from BioRad Laboratories (Richmond, CA), Streptavidin-biotinylated horseradish peroxidase from Amersham International (Coryton, Cardiff, UK), biotinylated anti-DNP antibody from Molecular Probes, Inc.(Eugene, OR), BioTrace PVDF transfer membrane (0.45 μm) from Pall Corporation (Ann Arbor, MI), X-ray film from Eastman Kodak Co. (Rochester, NY), and 8-isoprostane ELISA kit from Cayman Chemical Co. (Ann Arbor, MI).

Human HO-1 cDNA plasmid construction

An hHO-1 construct was prepared consisting of pcDNA3.1/Zeo CMV Flag hHO-1 containing the entire protein-coding region (866 bp) of the human HO-1 gene. Plasmid assembly was enabled using a forward primer (5′-TTC ATA CAA GCT TAT GGA GCG TCC GCA ACC-3′) containing a *Hind*III site and a reverse primer (5′-TCA ATG GAT CCT CAC ATG GCA TAA AGC CCT-3′) containing a *Bam*HI site designed to match the multiple cloning sites in pcDNA3.1/Zeo CMV Flag. The hHO-1 fragment was amplified by *pfu* DNA polymerase-catalyzed PCR and adenine overhangs were added to the PCR product with *Taq* DNA polymerase. After purification of the PCR products, the *Hind*III/*Bam*HI fragment of hHO-1 was subcloned into pGEM-T easy vector for color screening of recombinant clones. hHO-1 fragment (*Hind*III/*Bam*HI) was excised from recombinant pGEM-T by digestion with *Hind*III and *Bam*HI and inserted into the *Hind* III and *Bam*HI sites of pcDNA3.1/Zeo CMV Flag. Identical plasmids minus the hHO-1 cDNA were used for sham (control) transfections. Correct orientation and sequence of the hHO-1-Flag and Flag-only constructs were confirmed on sequencing gels.

Primary astrocyte cultures

Primary neuroglial cell cultures were prepared by mechanoenzymatic dissociation of cerebral tissue as previously described (Chopra et al., 1995). Cells were grown in Ham's F12 and high glucose DMEM (50:50 v/v) supplemented with 10 mM HEPES, 5% heat-inactivated horse serum, 5% heat-inactivated fetal bovine serum, and penicillin-streptomycin (50 U/ml and 50 μg/ml, respectively). Cells were seeded in T25 or T75 cm^2 tissue culture flasks at a density of 1×10^6 cells/ml. The cultures were incubated at 37°C in humidified 95% air–5% CO_2 for 6 h at which time they were vigorously shaken 20–30 times with replacement of fresh media to remove adherent oligodendroglia and microglia from the astrocytic monolayers. The cultures were incubated under the above-mentioned conditions for 6 days at which time more than 98% of the cells comprising the monolayer were astroglia as determined by immunohistochemical labeling for the astrocyte-specific marker, glial fibrillary acidic protein (GFAP) (Chopra et al., 1995). All drug treatments and gene transfections were initiated on in vitro day 7.

Transfection of human HO-1 cDNA

Upon reaching >90% confluence, 1×10^6 cells were transiently transfected with 0.5–6.0 μg of plasmid DNA-Lipofectamine 2000 complex using Lipofectamine 2000 method according to manufacturer instructions (Invitrogen). Plasmid DNA (0.5–6 μg) and 15 μl of Lipofectamine 2000 reagent were diluted individually in 250 μl opti-MEM I reduced serum medium and incubated for 5 min at room temperature with gentle mixing. The two solutions were combined, incubated at room temperature for 20 min to promote formation of DNA-lipid complexes and administered to the cells. Following incubation for 6 h at 37°C, the transfection mixture was replaced with complete media without antibiotics. At 12 h post-transfection, some cultures were treated with tin mesoporphyrin (SnMP; 1 μM), a competitive inhibitor of heme oxygenase activity (with light-shielding to prevent metalloporphyrin photoactivation). At concentrations below 5 μM, the metalloporphyrin specifically inhibits the enzymatic activity of heme oxygenase, but not nitric oxide synthase or other heme-containing enzymes (Appleton et al., 1999).

Cells were harvested at 72 h post-transfection for HO-1 mRNA/protein expression, HO enzyme activity, oxidative substrate damage, and viability/proliferation assays, as described below. Transfection efficiency was determined by assessment of green fluorescence protein (GFP) expression in astrocytes co-transfected with hHO-1 cDNA plasmid and pEGFP.C1 vector (Fig. 1). Briefly, the cells were seeded on coverslips coated with 1% gelatin. On day 3 post co-transfection with plasmids containing hHO-1 and EGFP (1:1), the coverslips were washed twice with PBS and mounted on glass slides with 95% glycerol +5% dH_2O. The transfection efficiency was ascertained by evaluation of nine coverslips in three separate experiments and expressed as number transfected cells (counted under FITC fluorescence)/total cells (counted under phase contrast) × 100%. The transfection efficiency was determined to be 42.1 ± 1.4% (mean ± SE).

Western blot analysis

Cells were rinsed twice with cold PBS (pH 7.4) and scraped in iced lysis buffer consisting of 1% Nonidet P-40, 50 mM Tris HCl (pH 7.4), 30 mM NaCl, 25 mM β-glycerophosphate, 10 mM EDTA, 10 mM EGTA, 1 mM $MgCl_2$, and protease inhibitors (10 mM sodium fluoride, 50 μg/ml AEBBSF, 5 μg/ml leupeptin, 5 μg/ml pepstatin, 5 μg/ml aprotinin). Supernatants were obtained by centrifugation at 15,000 rpm for 15 min at 4°C. Protein contents were determined using the Bradford method. Twenty μg aliquots plus 6× SDS–PAGE loading buffer (300 mM Tris HCl pH 6.8, 600 mM DTT, 12% SDS, 0.6% bromophenol blue, 60% glycerol) were subjected to 10% sodium dodecyl sulfate-polyacrylamide gel electrophoresis and transferred to the polyvinylidene fluoride membranes. Nonspecific binding was blocked by incubation in Tris buffer saline (pH 7.4) containing 3% nonfat milk and 0.1% Tween 20 for 1 h at room temperature. Blots were probed with mouse anti-Flag monoclonal antibody (1:200 diluted) and anti-β-actin monoclonal antibody (1:500 diluted). The secondary antibody consisted of horseradish peroxidase-conjugated goat anti-mouse antibody (1:4,000 dilution). Protein bands were visualized by enhanced chemiluminescence using ECL Western blotting reagents.

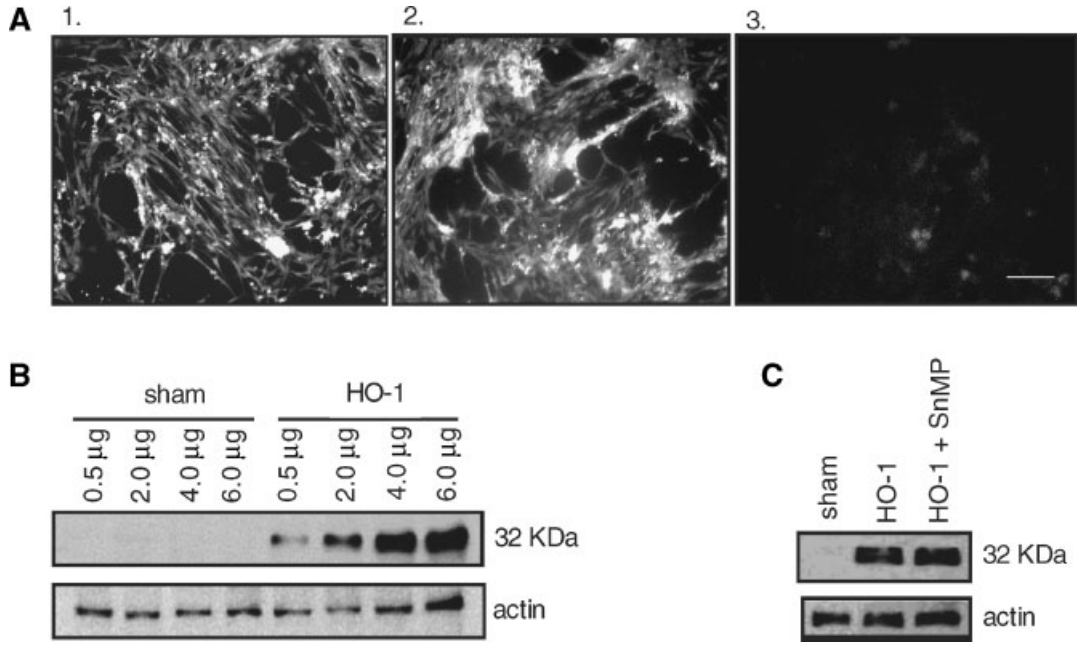

Fig. 1. **A**: Cytoplasmic expression of enhanced green fluorescent protein (EGFP) in astrocytes co-transfected with pcDNA3.1(+)/Zero Flag hHO-1 and pEGFP.C1 (1); pcDNA3.1(+)/Zero Flag and pEGFP.C1 (2); or pcDNA3.1(+)/Zero Flag hHO-1 only (control; (3)) Bar = 25 µm. **B**: Anti-Flag Western blotting for the detection of Flag-tagged hHO-1 protein in hHO-1 transfected and control astrocytes. **C**: Anti-Flag Western blotting for the detection of Flag-tagged hHO-1 protein in hHO-1-transfected, hHO-1-transfected/SnMP (1 µM)-treated, and sham-transfected astrocytes (4.0 µg plasmid DNA per 10^6 cells). All data were collected on post-transfection day 3.

HO enzyme activity assay

Cytosol extracts were prepared for HO activity measurement by the method of (Ryter et al., 2000). Cells were scraped in cold PBS-EDTA (1 mM, pH 8.0) containing 50 µg/ml protease inhibitor (AEBSF), centrifuged at 150*g* at 4°C and resuspended in 20 mM Tris-HCl (pH 7.4) and 0.25 M sucrose containing protease inhibitors. Cell suspensions were sonicated on ice 2×15 s at 20 W and centrifuged for 20 min at 4°C at 15,000*g*. Final reaction concentrations were 25 µM heme, 2 mM glucose 6-phosphate, 2 units glucose 6-phosphate dehydrogenase, 1 mM β-NADPH, 0.5 mg/ml cytosol extract, and 2 mg/ml partially purified rat liver biliverdin reductase. Reaction mixtures were incubated at 37°C in the dark for 60 min. The reactions were terminated by addition of 1 volume chloroform. Bilirubin concentrations in the chloroform extracts were determined spectrophotometrically by absorbance at 464–530 nm. HO activity was calculated as picomoles bilirubin per miligram protein per min, assuming an extinction coefficient of 40/mM/cm in chloroform.

Cell viability and proliferation

Cell viability was assessed by trypan blue exclusion as described by (Abraham et al., 1995) and using the mitochondria-based MTT assay as previously reported by our laboratory (Christodoulopoulos et al., 1999). Cell proliferation was determined by [^{3}H] thymidine incorporation and total cell counting: Astrocytes were plated in T25 flasks at 10^6 cells/ml in complete medium. [^{3}H] thymidine (1 µCi/ml) was added to the culture media for 20 h prior to cell harvesting. The cells were trypsinized, air-dried on 21 mm Ø glass microfibre filters (Whatman International Ltd., Maidstone, England) and analyzed by scintillation counting in a Wallac-Liquid Scintillator Counter (PerkinElmer Life Sciences, Boston, MA). [^{3}H] thymidine incorporation was expressed as counts per min (cpm) per ml. Cells in parallel flasks not receiving [^{3}H] thymidine were harvested by trypsinization and counted using a hemocytometer.

Subcellular fractionation

Subcellular fractionation was performed as previously described (Schipper et al., 1999). Briefly, cells were scraped, centrifuged and resuspended in 10 volumes of lysis buffer (Ponka et al., 1982) containing 4 mM $MgCl_2$, 2 mM Tris-HCl pH 7.4, and 1 mM AEBSF. The cells were sonicated (Sonics & Materials, Danbury, CT) at a power level of 50 for 3×20 s in a cooled water bath. Cell sonicates were suspended in 12.2% (v/v) Ficoll in 250 mM sucrose, 100 mM Tris-HCl pH 7.4 and 1 mM EDTA, and centrifuged at 55,000*g* for 40 min. The fractionation procedure results in ~65-fold enrichment for mitochondria as determined by cytochrome c oxidase assay (Schipper et al., 1999). Whole-cell and mitochondrial preparations were assayed for protein carbonyls, 8-*epi*$PGF_{2\alpha}$, and 8-hydroxy-2′-deoxyguanosine (8-OHdG) as described below.

Protein carbonyl assay

Protein carbonyl content, a widely-used measure of oxidative protein modification (Buss et al., 1997; Winterbourn and Buss, 1999), was determined by ELISA. Protein carbonyls were reacted with 2,4-dinitrophenylhydrazine (DNP) and the hydrazone adducts were detected with anti-DNP antisera. Quantification was achieved by comparison with oxidized BSA standards. Oxidized (carbonylated) BSA was prepared by reacting natural BSA (at 50 mg/ml in PBS) with hypochlorous acid (5 mM) for 1 h at 37°C, following by overnight dialysis against PBS at 4°C. Fully reduced BSA was prepared by reacting natural BSA (at 0.5 g/100 ml in PBS) with sodium borohydride (0.1 g) for 30 min at room temperature, followed by slow neutralization with 2 M HCl and overnight dialysis against PBS. DNP was combined with the BSA standards and carbonyl content determined colorimetrically by absorbance at 375 nm ($\varepsilon = 22{,}000$/M/cm) (Winterbourn and Buss, 1999). All samples were adjusted to 4.0 mg protein/ml. The standards and samples were incubated with 3 volumes of 10 mM DNP in 6 M guanidine-HCl and 0.5 M potassium phosphate (pH 2.5) for 45 min at room temperature with mixing every 10–15 min. Five microliters aliquots of each reaction mixture were mixed with 1 ml PBS and 200 µl replicates were added per well to 96-well immunoplates and incubated overnight at 4°C. After washing with PBS, nonspecific binding sites were blocked with 0.1% Tween 20 in PBS. Wells were incubated with biotinylated anti-DNP antibody (1:1,000 dilution in 0.1% Tween 20/PBS) for 1 h at 37°C followed by incubation with streptavidin-biotinylated horseradish peroxidase (1:3,000 dilution in 0.1% Tween

20/PBS). An o-phenylenediamine/peroxide solution (200 μl) was added to the reaction mixture for 4–7 min (terminated with 100μl of 2.5 M sulfuric acid) and read at 490 nm. A 6-point standard curve of reduced and oxidized BSA was generated for each plate analyzed. Specific absorbance for each sample was calculated by subtracting basal absorbance of the DNP reagent from the total absorbance.

8-epiPGF$_{2\alpha}$ assay

Concentrations of 8-*epi*PGF$_{2\alpha}$ (8-isoprostane), a highly specific marker of lipid peroxidation (Basu, 2003), were measured in culture media (free form), whole cells and mitochondrial fractions (membrane-bound and cytosolic forms) using an ELISA kit with a modified Sep-Pak procedure. This assay was based on competition between 8-isoprostane and an 8-isoprostane-acetylcholinesterase (AChE) conjugate (8-isoprostane tracer) for a limited number of 8-isoprostane-specific rabbit antiserum binding sites (Morrow and Roberts, 1991). For each culture sample, 10 ml of culture media were used and adjusted to pH 3.0 with acetic acid. Whole cell compartments and fractionated mitochondria were sonicated and treated with an equal volume of 15% KOH at 40°C for 1 h to hydrolyse and release esterified 8-isoprostanes. The samples were treated with two volumes of ethanol containing 0.05% BHT, vortexed and centrifuged to remove precipitated proteins. Ethanol was evaporated by vacuum centrifugation. Samples were adjusted to pH 4.0 with acetic acid. Sample purification was achieved by passing them through activated C_{18} SPE cartridges, washing with ultrapure water followed by HPLC grade hexane, and elution with 5 ml ethyl acetate containing 1% methanol. The eluates were vacuum-dried and dissolved in 450 μl of ELISA buffer and various dilutions were used for ELISA analysis (in triplicate). Technical controls: Wells for blanks (substrate only), non-specific binding (sample + tracer + substrate; no specific antibody to 8-*epi*PGF$_{2\alpha}$), maximum binding (tracer + specific antibody to 8-*epi*PGF$_{2\alpha}$ + substrate; no sample) and an eight-point standard curve (varying amounts of 8-*epi*PGF$_{2\alpha}$ standard provided in the kit + tracer + specific antibody to 8-*epi*PGF$_{2\alpha}$ + substrate) were set up in duplicate for each assay according to manufacturer instructions. Isoprostane levels were calculated and expressed as picogram 8-*epi*PGF$_{2\alpha}$/mg cell protein (cell lysates) or picogram 8-*epi*PGF$_{2\alpha}$/ml medium/mg protein (media).

8-hydroxy-2′-deoxyguanosine (8-OHdG) levels

Nuclear (n) and mitochondrial (mt) 8-OHdG levels, robust indices of oxidative nucleic acid damage (Helbock et al., 1999), were measured by HPLC with electrochemical detection (HPLC-ECD). nDNA or mtDNA were isolated by the chaotropic sodium iodide method (Helbock et al., 1999). All steps were performed at 4°C unless otherwise stated. The nDNA and mtDNA were hydrolyzed by digestion with nuclease P1 at 65°C for 11 min (Helbock et al., 1999). DNA was treated with calf alkaline phosphatase in Tris buffer (40 mM Tris-HCl, 10 mM $MgCl_2$, pH 8.5) for 60 min at 37°C and filtered through a 10,000-Da microfiltration tube (UltraFree, Millipore, Bedford, MA) for 45 min at 4°C. 8-OHdG and 2-deoxyguanosine (2-dG) were resolved and quantified by HPLC-ECD (Floyd et al., 1990) using a Waters millennium 32 system (996 photodiode array and pulsed electrochemical detectors, Milford, MA) with a 5 μm, 150 × 3.9 mm Atlantis C-18 column (Waters, Milford, MA). Nucleosides were eluted from the column with an isocratic mobile phase consisting of 50 mM potassium phosphate buffer (pH 5.5) and 4.0% acetonitrile that was filtered and degassed using a 0.22 μm nitrocellulose filter (Corning, NY) followed by sonication for 30 min. The oxidation potential of the electrochemical detector was set at 650 mV. The HPLC-ECD system was calibrated with 500 fmol–1 nmol of 8-OHdG and 5 nmol–10 μmol of 2-dG using authentic 8-OHdG and 2-dG standards (Sigma Chemical Co., St. Louis, MO). The data were expressed as the ratio of 8-OHdG (nmoles) to 2-dG (10^6 nmoles).

Statistics

All data in this study are presented as mean ± SE. Statistical analyses were performed by one-way ANOVA followed by Newman–Keuls posthoc comparisons to assess significant main effects within groups. Statistical significance was set at $P < 0.05$.

RESULTS

HO-1 expression and HO enzyme activity

Flag-tagged HO-1 protein was expressed in a dose-dependent manner on day 3 following transient transfection of primary rat astrocytes with pcDNA3.1/Zeo CMV Flag hHO-1 (0.5–6.0 μg of plasmid DNA per 10^6 cells; Fig. 1). In these cells, heme oxygenase activity increased 0.5–3.6 fold relative to sham-transfected controls in parallel with hHO-1 protein expression (Fig. 2). Administration of SnMP significantly attenuated heme oxygenase activity in the transfected cells (Fig. 2) without affecting the expression level of Flag-tagged HO-1 protein (Fig. 1).

Oxidative mitochondrial damage

(i) Protein oxidation: Transfection of hHO-1 significantly augmented the content of protein carbonyls in glial mitochondria and whole cell compartments in a dose dependent manner (Fig. 3). At the lowest dose tested (0.5 μg/10^6 cells), there was a significant increase in carbonyl content of mitochondria, but not whole cell compartments. Administration of SnMP significantly attenuated oxidative protein damage accruing from hHO-1 transfection in these cells (Fig. 3). (ii) Lipid peroxidation: In the mitochondrial fraction, the lowest hHO-1 plasmid DNA dose tested (0.5 μg per 10^6 cells) significantly reduced the concentration of 8-*epi*PGF$_{2\alpha}$ relative to control levels. In contrast, higher hHO-1 plasmid DNA doses ranging from 2.0 to 6.0 μg per 10^6 cells significantly augmented 8-*epi*PGF$_{2\alpha}$ concentrations in these organelles (Fig. 3). The hHO-1 transgene significantly increased concentrations of 8-*epi*PGF$_{2\alpha}$ in whole cell compartments at high plasmid DNA doses (4.0 and 6.0 μg per 10^6 cells) relative to control preparations, but had no effect on this lipid peroxidation marker in whole cells at lower doses (Fig. 3). hHO-1 transgene doses of 2.0 μg per 10^6 cells and higher also engendered significantly augmented 8-*epi*PGF$_{2\alpha}$ concentrations in the culture media in comparison with non- and sham-transfected controls (Fig. 3). Administration of SnMP (1 μM) abrogated the effects of hHO-1 transfection on 8-*epi*PGF$_{2\alpha}$ concentrations in astroglial

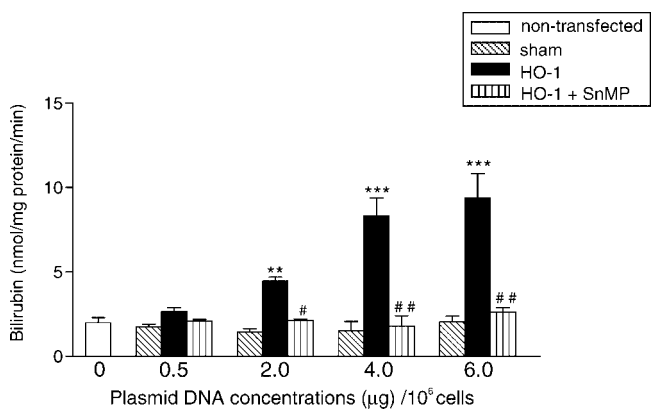

Fig. 2. Heme oxygenase activity in hHO-1-transfected and control astrocytes in the presence and absence of SnMP (1 μM). n = 4–6 sister cultures per experimental group. Data shown represent means ± SE. $^{**}P < 0.01$ and $^{***}P < 0.001$ relative to sham-transfected controls; $^{\#}P < 0.01$ and $^{\#\#}P < 0.001$ relative to hHO-1-transfected cells. All measurements were performed on post transfection day 3. The experiments depicted in Figures 2–5 were repeated at least three times with similar results on each occasion.

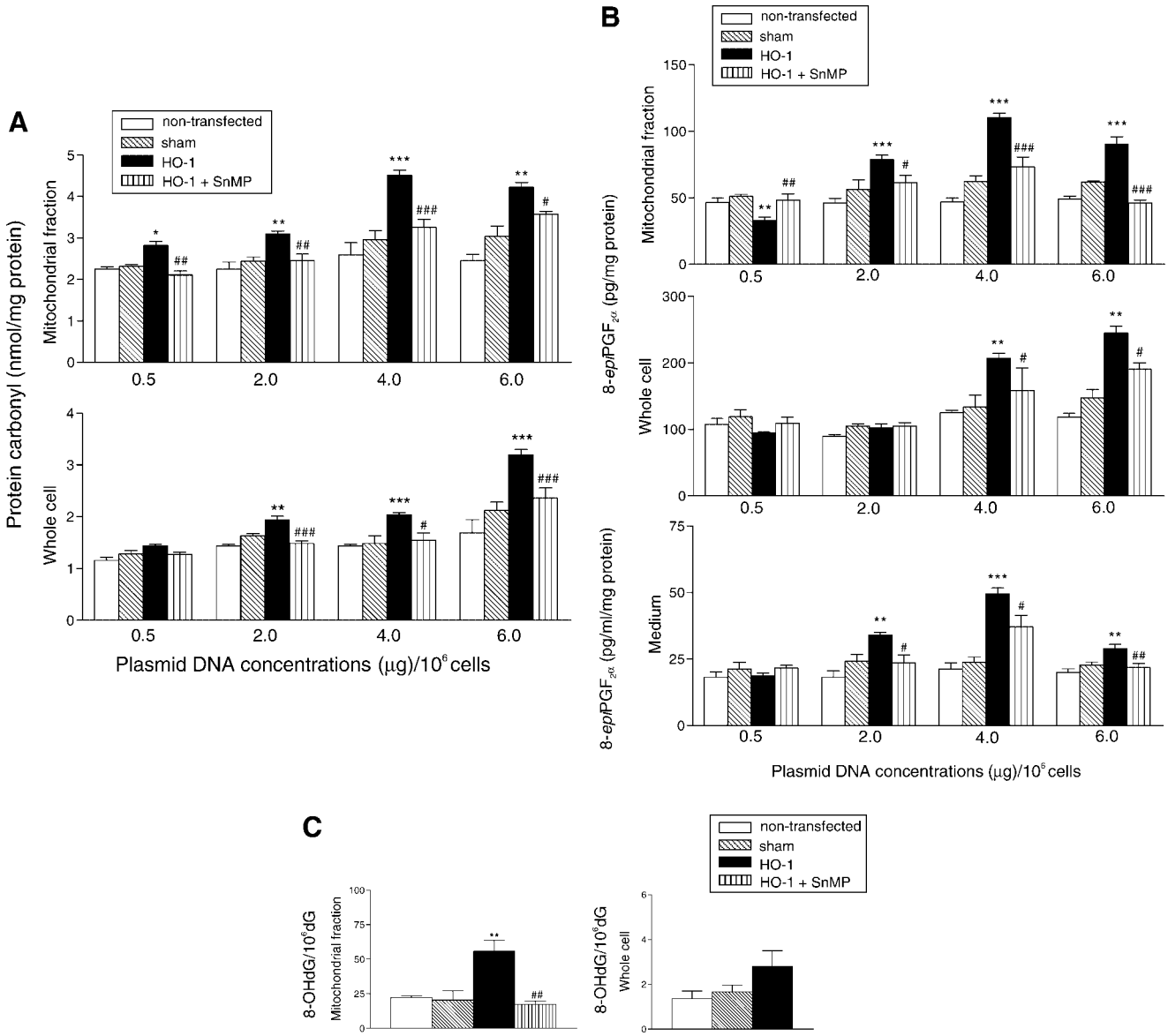

Fig. 3. Effects of hHO-1 transfection on markers of oxidative stress in cultured astroglia. **A**: Protein carbonyl content in non-transfected astroglia, sham-transfected astroglia and cells transfected with varying concentrations of hHO-1 plasmid DNA (0.5–6.0 μg per 10^6 cells) in the presence and absence of SnMP (1 μM). **B**: Concentrations of 8-*epi*$PGF_{2\alpha}$ in non-transfected astrocytes, sham-transfected astrocytes and cells transfected with varying concentrations of hHO-1 plasmid DNA (0.5–6.0 μg per 10^6 cells) in the presence and absence of SnMP (1 μM). **C**: 8-OHdG concentrations in non-transfected astrocytes, sham-transfected astrocytes, and cells transfected with hHO-1 (4.0 μg plasmid DNA per 10^6 cells) in the presence and absence of SnMP (1 μM). n = 4–6 sister cultures per experimental group. Data shown represent means ± SE. $^{*}P < 0.05$, $^{**}P < 0.01$, and $^{***}P < 0.001$ relative to sham-transfected controls; $^{\#}P < 0.05$, $^{\#\#}P < 0.01$, and $^{\#\#\#}P < 0.001$ relative to hHO-1-transfected cells. All measurements were made on post-transfection day 3.

mitochondrial fractions, whole cell compartments and culture media (Fig. 3). (iii) Oxidative DNA damage: Due to limitations in the amount of mitochondrial nucleic acids that can be extracted from primary glial monolayers for HPLC analysis, and the robust effects of 4 μg hHO-1 plasmid DNA per 10^6 cells on mitochondrial protein carbonylation and lipid peroxidation (Fig. 3), we selected this level of transfection alone to investigate the effects of hHO-1 on 8-OHdG concentrations in mitochondrial and whole cell compartments. As depicted in Fig. 3, hHO-1 transfection significantly increased 8-OHdG/dG ratios levels in mitochondrial fractions, but not whole cell compartments, relative to sham- and non-transfected preparations. As in the case of protein oxidation and lipid peroxidation, hHO-1-mediated oxidative nucleic acid damage was obviated by administration of 1 μM SnMP (Fig. 3).

Cell viability

Transfection of pcDNA3.1/Zeo CMV Flag hHO-1 (0.5–6.0 μg of plasmid DNA per 10^6 cells) in primary rat astroglia significantly increased cell death in a dose-dependent manner beginning at the hHO-1 plasmid DNA dose of 2.0 μg per 10^6 cells relative to sham-transfected controls (Fig. 4). However, hHO-1-dependent cell death in these preparations was relatively mild as indicated by both trypan blue exclusion and the MTT assay. Administration of 1 μM SnMP or the iron chelator, DFO (100 μM) significantly attenuated the effects of hHO-1 transfection on cell viability (Fig. 4).

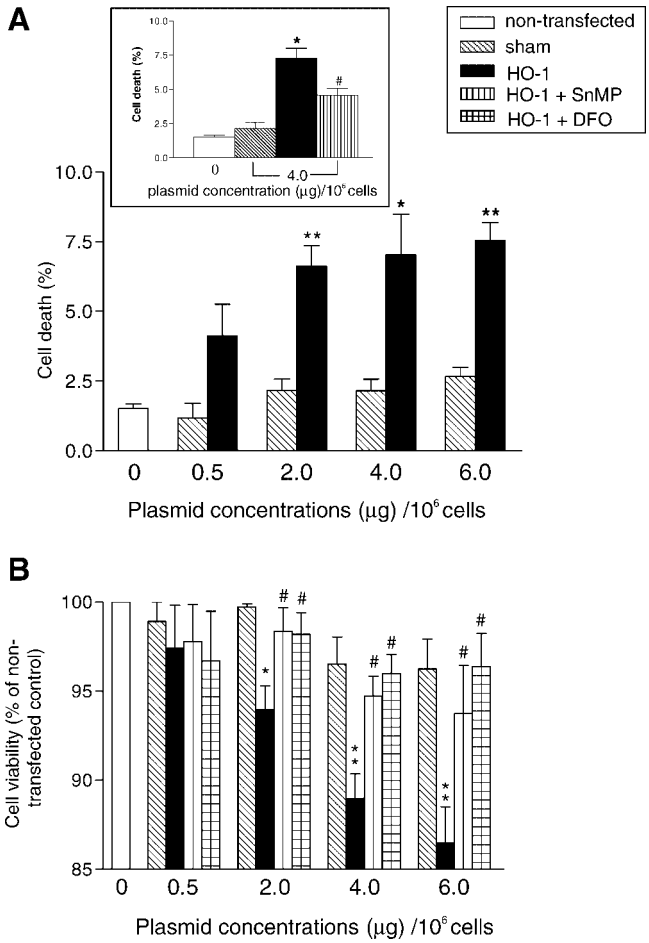

Fig. 4. Effects of hHO-1 transfection on astroglial viability. **A**: Viability of astrocytes transiently-transfected with hHO-1 or sham vector in the presence and absence of SnMP (1 μM) as determined by trypan blue exclusion. **B**: Cell viability of control and hHO-1-transfected cells in the presence and absence of SnMP (1 μM) or deferoxamine (100 μM) as determined by MTT assay. n = 4–6 sister cultures per experimental group. Data shown represent means ± SE. $^{*}P < 0.05$ and $^{**}P < 0.01$ relative to sham-transfected controls; $\#P < 0.05$ relative to hHO-1-transfected cells. All measurements were made on post-transfection day 3.

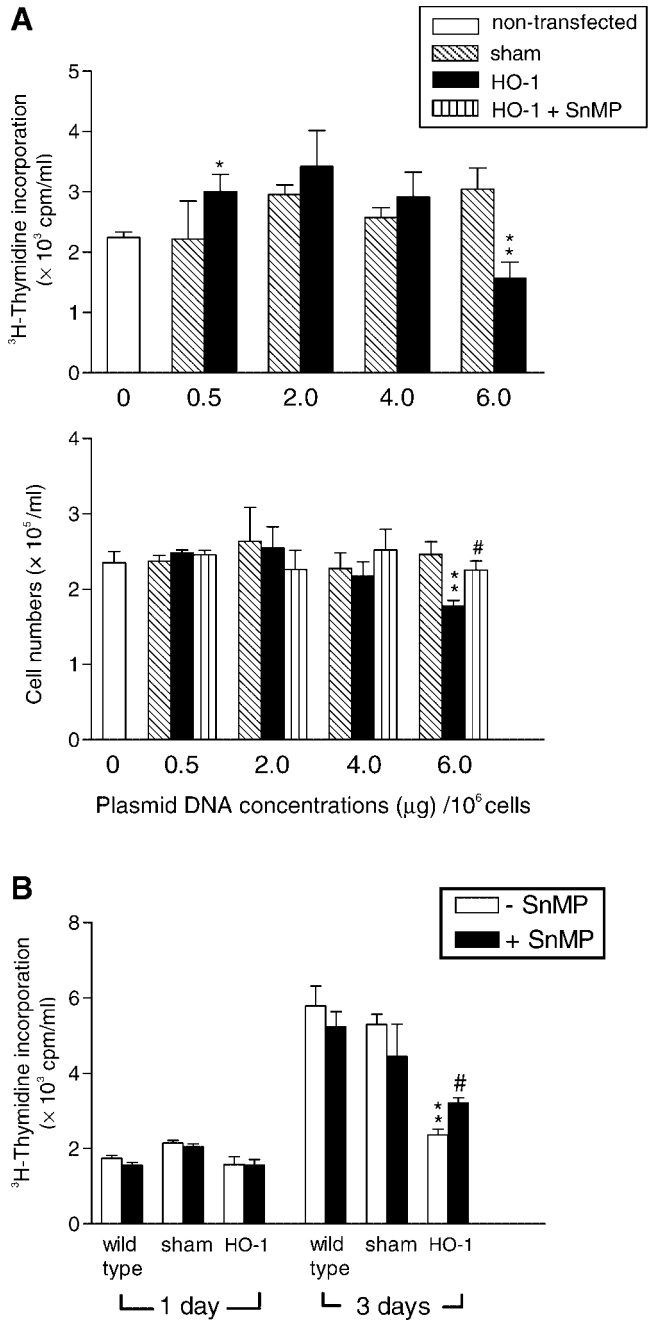

Fig. 5. Effects of hHO-1 transfection on glial ^{3}H-thymidine incorporation and cell numbers as a function of plasmid concentration (**A**) and duration of transfection (**B**) in the presence and absence of SnMP (1 μM). n = 4–6 sister cultures per experimental group. Data shown represent means ± SE. $^{*}P < 0.05$ and $^{**}P < 0.01$ relative to sham-transfected controls; $\#P < 0.05$ relative to hHO-1-transfected cells. Measurements shown in part A were performed on post-transfection day 3. hHO-1 transfections depicted in part B employed 6.0 μg plasmid DNA per 10^6 cells.

Cell proliferation

^{3}H-thymidine incorporation in rat astrocytes was significantly increased on day 3 following transfection with 0.5 μg hHO-1 cDNA/10^6 cells, significantly suppressed by transfection with 6.0 μg hHO-1 cDNA/10^6 cells and not affected by intermediate doses of hHO-1 cDNA (Fig. 5). Total cell numbers remained unchanged on day 3 following transfection with the 0.5 μg hHO-1 cDNA dose, were significantly reduced by transfection with 6.0 μg hHO-1 cDNA/10^6 cells and not affected by intermediate doses of hHO-1 cDNA (Fig. 5). On post-transfection day 3, SnMP (1 μM) significantly attenuated the inhibitory effects of hHO-1 transfection (6.0 μg plasmid DNA/10^6 cells) on ^{3}H-thymidine incorporation in these cells (Fig. 5). hHO-1 transfection (6.0 μg plasmid DNA/10^6 cells) and SnMP (1 μM) exposure had no appreciable affects on ^{3}H-thymidine incorporation at the 24 h time point (Fig. 5).

DISCUSSION

Over-expression of the human *ho-1* gene in cultured primary rat astroglia, corresponding to enhancement of bilirubin production in the range of 0.5–3.6 fold above control levels, resulted in robust oxidative damage to mitochondrial proteins, lipids and nucleic acids as evidenced, respectively, by significant increases in protein carbonyl, 8-*epi*$PGF_{2\alpha}$ and 8-OHdG concentrations in these organelles. At low-intermediate plasmid DNA concentrations, the hHO-1 transgene stimulated or exerted no effect on ^{3}H-thymidine incorporation in the cultured astroglia by post-transfection day 3 relative

to control values, whereas ^{3}H-thymidine incorporation and total cell numbers were significantly suppressed at higher levels of hHO-1 expression. The redox perturbations and altered patterns of growth/viability observed in our hHO-1 transfected astroglia were significantly attenuated by administration of 1 μM SnMP, attesting to the biological potency of the *hho-1* gene product in these preparations. Our current observations are consistent with earlier reports indicating that the proliferative response of cells in culture to oxidative stress is often bimodal, with enhanced proliferation accruing from relatively mild oxidative stress followed by arrested growth and augmented cell death at more intense levels of exposure (Davies, 1999; Droge, 2002). The effects of HO-1 over-expression in primary rat astroglia are akin to the anti-proliferative and pro-apoptotic effects of HO-1 previously reported in cultured fibroblasts, certain epithelial cells (Durante, 2003), vascular smooth muscle cells (Duckers et al., 2001; Tulis et al., 2001; Liu et al., 2002; Peyton et al., 2002), and testicular germ cells (Ozawa et al., 2002). In contrast, we recently observed that analogous levels of hHO-1 induction consistently stimulate proliferation and suppress indices of mitochondrial oxidation and cell death in C6 rat glioma and M17 human neuroblastoma cell lines (Song, Su, Song, Paudel and Schipper, unpublished results), similar to the predominantly pro-proliferative effects of HO-1 described in other tumor cells (Maines and Abrahamsson, 1996), in endothelial cells during angiogenesis (Deramaudt et al., 1998), and in keratinocytes (Clark et al., 1997). These disparate findings further attest to the fact that the primary heme metabolites, ferrous iron, CO, and biliverdin/bilirubin, may differentially impact pathways subserving cell cycle traverse and apoptosis in a cell type-specific manner (Durante, 2003).

The Janus-faced behavior of HO-1 in cellular redox homeostasis, growth and viability may explain the conflicting reports of the enzyme's contribution to tissue survival and lesion size in various experimental models of neural injury and disease: HO-1 over-expression has been shown to confer neuroprotection to cultured cerebellar granule cells exposed to excitotoxins (Chen et al., 2000), to neuroblastoma cells treated with ß-amyloid or H_2O_2 (Le et al., 1999; Takeda et al., 2000), and in the intact rodent brain following ischemic or traumatic insult (Maines et al., 1998). On the other hand, metalloporphyrin suppression of heme oxygenase activity was noted to ameliorate tissue necrosis and edema after focal cerebral ischemia in intact rats (Kadoya et al., 1995), neuronal injury, cerebral cavitation or edema in animal models of intracerebral hemorrhage (Wagner et al., 2000; Huang et al., 2002; Koeppen et al., 2004), superficial siderosis in rabbits following experimental subarachnoid hemorrhage (Koeppen and Dickson, 2002), and traumatic CA1 damage in rat hippocampal slices (Panizzon et al., 1996). The magnitude and duration of HO-1 induction, the status of the local redox microenvironment, engagement of disease-specific pathophysiological pathways, differences in species, strain, age and gender, and other protocol variations have been cited as possible explanations for the disparate behavior of HO-1 in neural tissues (Ryter and Tyrrell, 2000). Given the marked cellular heterogeneity of the mammalian brain, and in light of the present findings, it is conceivable that, within a given neuropathological state, up-regulation of HO-1 may protect one cellular compartment (e.g., neurons) while simultaneously compromising another (astrocytes).

The propensity for HO-1 activity to exacerbate oxidative stress in astroglial mitochondria may figure centrally in the pathogenesis of several degenerative and inflammatory human neurological conditions. Relative to control tissues, marked increases in astroglial HO-1 immunoreactivity have been reported in AD temporal cortex and hippocampus (Schipper et al., 1995), the substantia nigra of subjects with idiopathic PD (Schipper et al., 1998), MS plaques (Mehindate et al., 2001), and the peri-infarctional zones of patients with ischemic stroke (Beschorner et al., 2000). Studies conducted in our laboratory indicate that the up-regulation of HO-1 in astroglia may contribute to the pathological deposition of redox-active iron and bioenergetic failure (mitochondrial insufficiency) that have been amply documented in these CNS disorders (Schipper, 2004b). In primary rat astroglial cultures, exogenous β-amyloid $_{40/42}$ (deposited in AD brain), dopamine (released from dying nigrostriatal neurons in PD), and Th1 cytokines (secreted within MS plaques) up-regulate HO-1 mRNA, protein and/or activity levels within 3–12 h of treatment. Within 3–6 days of exposure to these stimuli, sequestration of non-transferrin-derived ^{59}Fe (or ^{55}Fe) by the mitochondrial compartment is significantly augmented in these cells (Schipper, 1999; Ham and Schipper, 2000; Mehindate et al., 2001). These treatments had no detectable effect on mitochondrial trapping of diferric transferrin-derived iron (*ibid.*), an observation commensurate with the fact that brain iron deposition under various neuropathological conditions in situ occurs independently of transferrin and its receptor (Schipper, 2000). Co-administration of SnMP or dexamethasone, a transcriptional suppressor of the *ho-1* gene, significantly attenuated mitochondrial iron sequestration in cultured astrocytes exposed to DA, β-amyloid, TNFα or IL-1β. Similarly, administration of SnMP or dexamethasone abolished the pathological accumulation of mitochondrial ^{55}Fe observed in rat astroglia engineered to over-express the *hho-1* gene by transient transfection (Schipper, 1999; Ham and Schipper, 2000; Mehindate et al., 2001). These findings indicate that up-regulation of HO-1 is a pivotal event leading to excessive mitochondrial iron deposition in chemically-stressed astroglia. In a previous study, we showed that treatment with ascorbate, melatonin, or resveratrol (potent natural antioxidants) blocked the late, compensatory induction of the *mnsod* gene in astrocytes transiently transfected with hHO-1 cDNA (Frankel et al., 2000). The latter observation raised the possibility that HO-1 up-regulation in astroglia, in contradistinction to other neural and non-neural tissues, promotes intracellular oxidative stress. The results of the present study, viz, augmentation of mitochondrial protein carbonyl, isoprostane and 8-OHdG levels in hHO-1-transfected astrocytes, constitute direct evidence in support of this formulation and implicate the mitochondrial compartment as a sensitive subcellular target of HO-1-mediated oxidative stress. Intracellular free ferrous iron and CO liberated in the course of HO-1-catalyzed heme degradation are likely mediators of oxidative mitochondrial injury in this paradigm (Zhang and Piantadosi, 1992) (Fig. 4B of present study; DFO effects). Of note, treatment with cyclosporin A or trifluoperazine, potent inhibitors of the mitochondrial permeability transition pore, curtailed mitochondrial iron trapping in hHO-1 transfected astroglia and cells exposed to DA, TNFα or IL-1β (Schipper, 1999; Mehindate et al., 2001). Conceivably, intracellular oxidative stress resulting from HO-1

activity promotes pore opening (Petronilli et al., 1993) and influx of cytosolic iron to the mitochondrial matrix. Engagement of the permeability pore and other redox-sensitive membrane channels may also permit egress of pro-apoptotic factors, such as cytochrome c, from mitochondria to the cytosol thereby facilitating the activation of effector caspases and apoptotic cell death. This would account for the correlation of growth arrest and increased cell death with enhanced markers of oxidative mitochondrial damage in the hHO-1 transfected astroglia. A densitometric analysis of HO-1 immunoblots performed on human brain lysates revealed approximately 2.4- and 5.8-fold increases in HO-1 expression in AD hippocampus and temporal cortex, respectively, relative to neurohistologically-normal (control) preparations matched for age and post-mortem interval (Schipper et al., 1995). The magnitude of HO-1 over-expression in AD brain is commensurate with the range of experimental HO augmentation achieved in the current study suggesting that the pathophysiological effects observed in the hHO-1 transfected astroglia are germane to events prevailing in AD-affected neural tissues.

In the diseased CNS, gliopathic changes characterized by oxidative mitochondrial damage and iron deposition may have secondary, deleterious effects on nearby neuronal constituents and other cellular compartments. For example, the glial mitochondrial iron catalyzes the bio-activation of the catechols, dopamine and 2-hydroxyestradiol to highly reactive o-semiquinone radicals, and the pro-toxin, MPTP to the potent neurotoxin, MPP+ (Schipper, 1999). Both MPP+ (Schipper, 1999) and superoxide anion derived from the redox cycling of o-semiquinones (Kontos et al., 1985) may be extruded to the extracellular space and exert direct dystrophic effects on susceptible neuronal targets. Furthermore, diminished ATP levels accruing from glial bioenergetic failure may predispose to neuronal degeneration by (i) augmenting extracellular glutamate concentrations (excitotoxicity) and (ii) curtailing GSH delivery to the neuronal compartment (Aschner, 2000). Targeted suppression of glial HO-1 hyperactivity in human neurodegenerative and inflammatory disorders may have important clinical implications because an *enzymatic* (HO-1) basis for oxidative mitochondrial injury may prove to be considerably more amenable to therapeutic intervention than free radical damage accruing from unregulated chemical processes (Droge, 2002).

ACKNOWLEDGMENTS

The authors thank Adrienne Liberman for excellent technical assistance.

LITERATURE CITED

Abraham N, Lavrovsky Y, Schwartzman M, Stoltz R, Levere R, Gerritsen M, Shibahara S, Kappas A. 1995. Transfection of the human heme oxygenase gene into rabbit coronary microvessel endothelial cells: Protective effect against heme and hemoglobin toxicity. Proc Natl Acad Sci USA 92:6798–6802.

Appleton SD, Chretien ML, McLaughlin BE, Vreman HJ, Stevenson DK, Brien JF, Nakatsu K, Maurice DH, Marks GS. 1999. Selective inhibition of heme oxygenase, without inhibition of nitric oxide synthase or soluble guanylyl cyclase, by metalloporphyrins at low concentrations. Drug Metab Dispos 27:1214–1219.

Aschner M. 2000. Neuron-astrocyte interactions: Implications for cellular energetics and antioxidant levels. Neurotoxicology 21:1101–1107.

Baranano DE, Snyder SH. 2001. Neural roles for heme oxygenase: Contrasts to nitric oxide synthase. Proc Natl Acad Sci USA 98:10996–11002.

Basu S. 2003. Carbon tetrachloride-induced lipid peroxidation: Eicosanoid formation and their regulation by antioxidant nutrients. Toxicology 189:113–127.

Beschorner R, Adjodah D, Schwab JM, Mittelbronn M, Pedal I, Mattern R, Schluesener HJ, Meyermann R. 2000. Long-term expression of heme oxygenase-1 (HO-1, HSP-32) following focal cerebral infarctions and traumatic brain injury in humans. Acta Neuropathol (Berl) 100:377–384.

Buss H, Chan TP, Sluis KB, Domigan NM, Winterbourn CC. 1997. Protein carbonyl measurement by a sensitive ELISA method. Free Radic Biol Med 23:361–366.

Chen K, Gunter K, Maines MD. 2000. Neurons overexpressing heme oxygenase-1 resist oxidative stress-mediated cell death. J Neurochem 75:304–313.

Chopra VS, Chalifour LE, Schipper HM. 1995. Differential effects of cysteamine on heat shock protein induction and cytoplasmic granulation in astrocytes and glioma cells. Brain Res Mol Brain Res 31:173–184.

Christodoulopoulos G, Malapetsa A, Schipper H, Golub E, Radding C, Panasci LC. 1999. Chlorambucil induction of HsRad51 in B-cell chronic lymphocytic leukemia. Clin Cancer Res 5:2178–2184.

Clark JE, Green CJ, Motterlini R. 1997. Involvement of the heme oxygenase-carbon monoxide pathway in keratinocyte proliferation. Biochem Biophys Res Commun 241:215–220.

Davies KJ. 1999. The broad spectrum of responses to oxidants in proliferating cells: A new paradigm for oxidative stress. IUBMB Life 48:41–47.

Dennery PA. 2000. Regulation and role of heme oxygenase in oxidative injury. Curr Top Cell Regul 36:181–199.

Deramaudt BM, Braunstein S, Remy P, Abraham NG. 1998. Gene transfer of human heme oxygenase into coronary endothelial cells potentially promotes angiogenesis. J Cell Biochem 68:121–127.

Dore S, Takahashi M, Ferris CD, Zakhary R, Hester LD, Guastella D, Snyder SH. 1999. Bilirubin, formed by activation of heme oxygenase-2, protects neurons against oxidative stress injury. Proc Natl Acad Sci USA 96:2445–2450.

Droge W. 2002. Free radicals in the physiological control of cell function. Physiol Rev 82:47–95.

Duckers HJ, Boehm M, True AL, Yet SF, San H, Park JL, Clinton Webb R, Lee ME, Nabel GJ, Nabel EG. 2001. Heme oxygenase-1 protects against vascular constriction and proliferation. Natl Med 7:693–698.

Durante W. 2003. Heme oxygenase-1 in growth control and its clinical application to vascular disease. J Cell Physiol 195:373–382.

Ewing JF, Maines MD. 1995. Immunohistochemical localization of biliverdin reductase in rat brain: Age related expression of protein and transcript. Brain Res 672:29–41.

Floyd RA, West MS, Eneff KL, Schneider JE, Wong PK, Tingey DT, Hogsett WE. 1990. Conditions influencing yield and analysis of 8-hydroxy-2′-deoxyguanosine in oxidatively damaged DNA. Anal Biochem 188:155–158.

Frankel D, Mehindate K, Schipper HM. 2000. Role of heme oxygenase-1 in the regulation of manganese superoxide dismutase gene expression in oxidatively-challenged astroglia. J Cell Physiol 185:80–86.

Galbraith R. 1999. Heme oxygenase: Who needs it? Proc Soc Exp Biol Med 222:299–305.

Ham D, Schipper HM. 2000. Heme oxygenase-1 induction and mitochondrial iron sequestration in astroglia exposed to amyloid peptides. Cell Mol Biol (Noisy-le-grand) 46:587–596.

Helbock HJ, Beckman KB, Ames BN. 1999. 8-Hydroxydeoxyguanosine and 8-hydroxyguanine as biomarkers of oxidative DNA damage. Methods Enzymol 300:156–166.

Huang FP, Xi G, Keep RF, Hua Y, Nemoianu A, Hoff JT. 2002. Brain edema after experimental intracerebral hemorrhage: Role of hemoglobin degradation products. J Neurosurg 96:287–293.

Kadoya C, Domino EF, Yang GY, Stern JD, Betz AL. 1995. Preischemic but not postischemic zinc protoporphyrin treatment reduces infarct size and edema accumulation after temporary focal cerebral ischemia in rats. Stroke 26:1035–1038.

Koeppen AH, Dickson AC. 2002. Tin-protoporphyrin prevents experimental superficial siderosis in rabbits. J Neuropathol Exp Neurol 61:689–701.

Koeppen A, Dickson A, Smith J. 2004. Heme oxygenase in brain hemorrhage. The benefit of tin-mesoporphyrin. J Neuropathol Exp Neurol 63:587–597.

Kontos HA, Wei EP, Ellis EF, Jenkins LW, Povlishock JT, Rowe GT, Hess ML. 1985. Appearance of superoxide anion radical in cerebral extracellular space during increased prostaglandin synthesis in cats. Circ Res 57:142–151.

Kontos HA, Wei EP, Ellis EF, Jenkins LW, Povlishock JT, Rowe GT, Hess ML. 1985. Appearance of superoxide anion radical in cerebral extracellular space during increased prostaglandin synthesis in cats. Circ Res 57:142–151.

Le WD, Xie WJ, Appel SH. 1999. Protective role of heme oxygenase-1 in oxidative stress-induced neuronal injury. J Neurosci Res 56:652–658.

Liu XM, Chapman GB, Wang H, Durante W. 2002. Adenovirus-mediated heme oxygenase-1 gene expression stimulates apoptosis in vascular smooth muscle cells. Circulation 105:79–84.

Llesuy SF, Tomaro ML. 1994. Heme oxygenase and oxidative stress. Evidence of involvement of bilirubin as physiological protector against oxidative damage. Biochim Biophys Acta 1223:9–14.

Maines MD, Abrahamsson PA. 1996. Expression of heme oxygenase-1 (HSP32) in human prostate: Normal, hyperplastic, and tumor tissue distribution. Urology 47:727–733.

Maines MD, Polevoda B, Coban T, Johnson K, Stoliar S, Huang TJ, Panahian N, Cory-Slechta DA, McCoubrey WK, Jr. 1998. Neuronal overexpression of heme oxygenase-1 correlates with an attenuated exploratory behavior and causes an increase in neuronal NADPH diaphorase staining. J Neurochem 70:2057–2069.

Matsuoka Y, Kitamura Y, Okazaki M, Kakimura J, Tooyama I, Kimura H, Taniguchi T. 1998. Kainic acid induction of heme oxygenase in vivo and in vitro. Neuroscience 85:1223–1233.

Mehindate K, Sahlas DJ, Frankel D, Mawal Y, Liberman A, Corcos J, Dion S, Schipper HM. 2001. Proinflammatory cytokines promote glial heme oxygenase-1 expression and mitochondrial iron deposition: Implications for multiple sclerosis. J Neurochem 77:1386–1395.

Morrow JD, Roberts LJ, 2nd. 1991. Quantification of noncyclooxygenase derived prostanoids as a marker of oxidative stress. Free Radic Biol Med 10:195–200.

Nakagami T, Toyomura K, Kinoshita T, Morisawa S. 1993. A beneficial role of bile pigments as an endogenous tissue protector: Anti-complement effects of biliverdin and conjugated bilirubin. Biochim Biophys Acta 1158:189–193.

Ozawa N, Goda N, Makino N, Yamaguchi T, Yoshimura Y, Suematsu M. 2002. Leydig cell-derived heme oxygenase-1 regulates apoptosis of premeiotic germ cells in response to stress. J Clin Invest 109:457–467.

Panizzon KL, Dwyer BE, Nishimura RN, Wallis RA. 1996. Neuroprotection against CA1 injury with metalloporphyrins. Neuroreport 7:662–666.

Petronilli V, Cola C, Massari S, Colonna R, Bernardi P. 1993. Physiological effectors modify voltage sensing by the cyclosporin A-sensitive permeability transition pore of mitochondria. J Biol Chem 268:21939–21945.
Peyton KJ, Reyna SV, Chapman GB, Ensenat D, Liu XM, Wang H, Schafer AI, Durante W. 2002. Heme oxygenase-1-derived carbon monoxide is an autocrine inhibitor of vascular smooth muscle cell growth. Blood 99:4443–4448.
Ponka P, Wilczynska A, Schulman HM. 1982. Iron utilization in rabbit reticulocytes. A study using succinylacetone as an inhibitor or heme synthesis. Biochim Biophys Acta 720:96–105.
Ryter SW, Tyrrell RM. 2000. The heme synthesis and degradation pathways: Role in oxidant sensitivity. Heme oxygenase has both pro- and antioxidant properties. Free Radic Biol Med 28:289–309.
Ryter SW, Kvam E, Tyrrell RM. 2000. Heme oxygenase activity. Current methods and applications. Methods Mol Biol 99:369–391.
Scapagnini G, D'Agata V, Calabrese V, Pascale A, Colombrita C, Alkon D, Cavallaro S. 2002. Gene expression profiles of heme oxygenase isoforms in the rat brain. Brain Res 954:51–59.
Schipper HM. 1999. Glial HO-1 expression, iron deposition and oxidative stress in neurodegenerative diseases. Neurotox Res 1:57–70.
Schipper HM. 2000. Heme oxygenase-1: Role in brain aging and neurodegeneration. Exp Gerontol 35:821–830.
Schipper H. 2004a. Glial heme oxygenase-1 in CNS injury and disease. In: Hertz L, editor. Non-neuronal cells of the nervous system: Function and dysfunction. Amsterdam: Elsevier. pp 869–882.
Schipper HM. 2004b. Heme oxygenase-1: Transducer of pathological brain iron sequestration under oxidative stress. In: LeVine S, Connor JR, Schipper HM, editors. Redox-active metals in neurological disorders. New York: Ann NY: Acad Sci. pp 84–93.
Schipper HM, Cissé S, Stopa EG. 1995. Expression of heme oxygenase-1 in the senescent and Alzheimer-diseased brain. Ann Neurol 37:758–768.
Schipper HM, Liberman A, Stopa EG. 1998. Neural heme oxygenase-1 expression in idiopathic Parkinson's disease. Exp Neurol 150:60–68.
Schipper HM, Bernier L, Mehindate K, Frankel D. 1999. Mitochondrial iron sequestration in dopamine-challenged astroglia: Role of heme oxygenase-1 and the permeability transition pore. J Neurochem 72:1802–1811.
Stocker R, Yamamoto Y, McDonagh AF, Glazer AN, Ames BN. 1987. Bilirubin is an antioxidant of possible physiological importance. Science 235:1043–1046.
Takeda A, Perry G, Abraham NG, Dwyer BE, Kutty RK, Laitinen JT, Petersen RB, Smith MA. 2000. Overexpression of heme oxygenase in neuronal cells, the possible interaction with Tau. J Biol Chem 275:5395–5399.
Tulis DA, Durante W, Liu X, Evans AJ, Peyton KJ, Schafer AI. 2001. Adenovirus-mediated heme oxygenase-1 gene delivery inhibits injury-induced vascular neointima formation. Circulation 104:2710–2715.
Wagner KR, Hua Y, de Courten-Myers GM, Broderick JP, Nishimura RN, Lu SY, Dwyer BE. 2000. Tin-mesoporphyrin, a potent heme oxygenase inhibitor, for treatment of intracerebral hemorrhage: In vivo and in vitro studies. Cell Mol Biol (Noisy-le-grand) 46:597–608.
Winterbourn CC, Buss IH. 1999. Protein carbonyl measurement by enzyme-linked immunosorbent assay. Methods Enzymol 300:106–111.
Zhang J, Piantadosi CA. 1992. Mitochondrial oxidative stress after carbon monoxide hypoxia in the rat brain. J Clin Invest 90:1193–1199.